Neurotoxicology 94 (2023) 35–45

Contents lists available at ScienceDirect

Neurotoxicology

journal homepage: www.elsevier.com/locate/neuro

Organophosphate insecticides disturb neuronal network development and function via non-AChE mediated mechanisms

Lennart V.J. van Melis [a,1], Harm J. Heusinkveld [a,b,2,1], Celine Langendoen [a], Anouk Peters [a], Remco H.S. Westerink [a,*]

[a] Neurotoxicology Research Group, Division of Toxicology, Institute for Risk Assessment Sciences (IRAS), Faculty of Veterinary Medicine, Utrecht University, P.O. Box 80.177, NL-3508 TD Utrecht, The Netherlands

[b] Centre for Health Protection, National Institute for Public Health and the Environment (RIVM), Bilthoven, The Netherlands

ARTICLE INFO

Keywords:
Microelectrode array (MEA)
In vitro hazard characterisation
Calcium imaging
Neuronal activity
Acute and developmental exposure
Organophosphate insecticides

ABSTRACT

Exposure to organophosphate (OP) insecticides has been related to several adverse health effects, including neurotoxicity. The primary insecticidal mode of action of OP insecticides relies on (irreversible) binding to acetylcholine esterase (AChE), with –oxon metabolites having a much higher potency for AChE inhibition than the parent compounds. However, OP insecticides can also have non-AChE-mediated effects, including changes in gene expression, neuroendocrine effects, disruption of neurite outgrowth and disturbance of the intracellular calcium (Ca^{2+}) homeostasis. Since Ca^{2+} is involved in neurotransmission and neuronal development, our research aimed to assess the effects of two widely used OP insecticides, chlorpyrifos (CPF) and diazinon (DZ) and their respective -oxon metabolites, on intracellular Ca^{2+} homeostasis in human SH-SY5Y cells and rat primary cortical cultures. Furthermore, we assessed the acute and chronic effects of exposure to these compounds on neuronal network maturation and function in rat primary cortical cultures using microelectrode array (MEA) recordings. While inhibition of AChE appears to be the primary mode of action of oxon-metabolites, our data indicate that both parent OP insecticides (CPF and DZ) inhibit depolarization-evoked Ca^{2+} influx and neuronal activity at concentrations far below their sensitivity for AChE inhibition, indicating that inhibition of voltage-gated calcium channels is a common mode of action of OP insecticides. Notably, parent compounds were more potent than their oxon metabolites, with exposure to diazinon-oxon (DZO) having no effect on both neuronal activity and Ca^{2+} influx. Human SH-SY5Y cells were more sensitive to OP-induced inhibition of depolarization-evoked Ca^{2+} influx than rat cortical cells. Acute exposure to OP insecticides had more potent effects on neuronal activity than on Ca^{2+} influx, suggesting that neuronal activity parameters are especially sensitive to OP exposure. Interestingly, the effects of DZ and chlorpyrifos-oxon (CPO) on neuronal activity lessened after 48 h of exposure, while the potency of CPF did not differ over time. This suggests that neurotoxicity after exposure to different OPs has different effects over time and occurs at levels that are close to human exposure levels. In line with these results, chronic exposure to CPF during 10 days impaired neuronal network development, illustrating the need to investigate possible links between early-life OP exposure and neurodevelopmental disorders in children and highlighting the importance of non-AChE mediated mechanisms of neurotoxicity after OP exposure.

1. Introduction

Pesticides are widely used in agricultural (professional) and indoor (household) applications to control various types of pests including plants, insects and rodents (Casida, 2017; Richardson et al., 2019). Exposure to pesticides has been related to several adverse health effects, including neurotoxicity in the developing and the adult brain (Chin-Chan et al., 2015; Kim et al., 2017; Mostafalou and Abdollahi, 2017; Naughton and Terry, 2018). A well-known class of widely used pesticides consists of the organophosphate (OP) insecticides. The primary

* Corresponding author.
E-mail address: R.Westerink@uu.nl (R.H.S. Westerink).
[1] both authors contributed equally.
[2] Present address: Centre for Health Protection, National Institute for Public Health and the Environment (RIVM), Bilthoven, The Netherlands.

https://doi.org/10.1016/j.neuro.2022.11.002

Available online 5 November 2022

insecticidal mode of action of organophosphate insecticides relies on (irreversible) binding to acetylcholine esterase (AChE), resulting in inhibition of acetylcholine hydrolysis, thereby causing a potentially lethal over-excitation of cholinergic neurotransmission (Casida, 2017; Naughton and Terry, 2018; Richardson et al., 2019). Symptoms of acute human OP intoxication can include sweating, gastrointestinal symptoms, respiratory depression, cardiovascular problems, convulsions and coma (Richardson et al., 2019; Tsai and Lein, 2021). Inhibition of AChE can also affect hormonal regulation impulses and thus function as an endocrine disruptor. Furthermore, exposure to the OP-insecticide chlorpyrifos can alter the levels of the sex hormones estrogen and androgen and increases stress hormone levels by activation of the hypothalamic-pituitary-adrenal axis (Ubaid ur Rahman et al., 2021). Effects of long-term exposure to OP-insecticides are still elusive, although long-term exposure has been associated with neurodegenerative diseases (Chin-Chan et al., 2015; Goldman, 2014; Sensi et al., 2017).

Toxicity of OP-insecticides is generally attributed to their primary –oxon metabolites since these metabolites have a higher potency for AChE inhibition than the parent compounds (Casida, 2017; Kasteel et al., 2020). However, non-AChE-mediated effects of the parent compounds and -oxon metabolites have been described for several OP-insecticides including parathion, chlorpyrifos (CPF), and diazinon (DZ). These non-AChE-mediated effects include disturbance of the intracellular calcium (Ca^{2+}) homeostasis, noradrenergic neurotransmission and differentiation of neuronal cells (Meijer et al., 2014a; Sidiropoulou et al., 2009; Slotkin et al., 2017; Tsai and Lein, 2021) at concentrations comparable with human occupational exposure levels. In addition, several in vitro and in vivo studies have shown that OP-insecticides can induce developmental neurotoxicity (Christen et al., 2017; Das and Barone, 1999; Oliveri et al., 2015; Todd et al., 2020; Zhang et al., 2015). Changes in expression of genes associated with neurotransmission have been found in rats after chronic and low-level exposure to DZ (Savy et al., 2018). CPF and DZ have also been shown to affect the adenylyl cyclase transduction pathway, which regulates proliferation and differentiation of neurons (Flaskos and Sachana, 2011). Both CPF, DZ and their oxon-metabolites (chlorpyrifos-oxon (CPO) and diazinon-oxon (DZO)) can disrupt neurite outgrowth (Flaskos, 2012; Pizzurro et al., 2014). Furthermore, chronic in vitro exposure to CPF and CPO has been shown to inhibit neuronal activity in rat cortical cells (Dingemans et al., 2016). Finally, exposure to CPF and CPO can decrease the transport of membrane bound organelles in cortical axons, which can impair neuronal development and function (Gao et al., 2017).

Disturbance of intracellular Ca^{2+} homeostasis is of particular concern since Ca^{2+} is involved in several essential neurobiological processes, including neurotransmission and neuronal development. In the presynaptic terminal, opening of voltage-gated calcium channels (VGCCs) triggers the subsequent release of neurotransmitter in the synaptic cleft (Dolphin and Lee, 2020). Since OP-insecticides are known to affect intracellular Ca^{2+} homeostasis and act on these VGCCs (Meijer et al., 2014a) they can affect neuronal function. Changes in Ca^{2+} homeostasis after exposure to these compounds can be recorded using real-time, fluorescent Ca^{2+} imaging, whereas effects on neuronal (network) function can be measured using for example multi-well microelectrode array (MEA) recordings.

A MEA consists of a cell culture surface with an integrated array of microelectrodes, which enables recording of extracellular field potentials generated by spontaneous neuronal activity of the cultured cells. Currently, rat primary cortical cells are the most widely used model for MEA recordings. Rat primary cortical cultures provide a heterogeneous in vitro model comprising multiple neural cell types (diverse subtypes of neurons and glial cells such as astrocytes) and thus a multitude of molecular targets, including VGCCs (Hondebrink et al., 2016; Tukker et al., 2020). In addition, the combined presence of stimulatory (glutamatergic) and inhibitory (GABAergic) neurons results in a spontaneously (electrically) active neuronal network that develops synchronized networks bursting (Cotterill et al., 2016; Robinette et al., 2011). Neuronal activity of rat cortical cells has been shown to be affected by different physiological, toxicological, and pharmacological compounds (Kosnik et al., 2020; Strickland et al., 2018). As such, MEA recordings cover multiple relevant mechanisms important for neuronal function, have a considerable throughput and high sensitivity and specificity. Also, MEA recordings are non-invasive, allowing for effect assessment at several timepoints during network development. Consequently, MEA recordings are increasingly used as a screening tool to investigate the acute and developmental neurotoxicity of chemicals (Gerber et al., 2021; Hogberg et al., 2011; McConnell et al., 2012; Tukker et al., 2020).

In addition to rat primary cortical cultures, we also used human SH-SY5Y cells (Biedler et al., 1973) to assess the effects of the test compounds on intracellular Ca^{2+} homeostasis. The SH-SY5Y cell provides a well-characterized catecholaminergic neuroblastoma cell line from human origin, widely used to study neurotoxicity in vitro (Heusinkveld and Westerink, 2017; Lopez-Suarez et al., 2022). Importantly, the parallel use of human SH-SY5Y cells and rat primary cortical cultures allows for assessing interspecies differences as well as assessment of integrated effect of OP-induced changes in Ca^{2+} homeostasis on network function. To explore the non-AChE-mediated effects of OP-insecticides, we investigated the effects of two widely used organophosphate insecticides, chlorpyrifos and diazinon, and their respective -oxon metabolites (Fig. 1) on intracellular Ca^{2+} homeostasis and cell viability in human SH-SY5Y cells and rat primary cortical cultures. Furthermore, we assessed the effects of acute and chronic exposure to these compounds on neuronal network development and activity in rat primary cortical cultures using MEA recordings.

2. Materials and methods

2.1. Chemicals

Fura-2-AM was obtained from Molecular Probes (Invitrogen, Breda, The Netherlands). Chlorpyrifos (CPF) (diethyl-(3,5,6-trichloropyridin-2-yl)-phosphate; CAS nr. 2921–88–2) and Diazinon (DZ) (O,O-Diethyl-O-(2-isopropyl-6-methyl-4-pyrimidinyl)-phosphorothioate; CAS nr. 333–41–5) were obtained Pestanal® grade, 99.8% purity (Riedel de Haën, Seelze, Germany). Chlorpyrifos-oxon (CPO) (CAS nr. 5598–15–2) was obtained from AccuStandard (New Haven, USA; purity 93.5%). Diazinon-oxon (DZO) (CAS nr. 962–85–3) was obtained from Chem Service Inc (West Chester, PA, USA; purity 97.3%). Unless otherwise noted, all other chemicals were obtained from Sigma Aldrich (Zwijndrecht, The Netherlands).

Saline solutions, containing (in mM) 125 NaCl, 5.5 KCl, 2 $CaCl_2$, 0.8 $MgCl_2$, 10 HEPES, 24 glucose and 36.5 sucrose (pH 7.3, adjusted using HCl), were prepared with de-ionized water (Milli-Q®). Stock solutions of 0.1–100 mM pesticide were prepared in DMSO and diluted in saline (Ca^{2+} imaging) or culture medium (MEA recordings, cell viability) just prior to the experiments. All solutions used in experiments, including control experiments, contained 0.1% DMSO.

2.2. Cell culture

Human SH-SY5Y cells (kindly provided by Dr. R. van Kesteren (Center for Neurogenomics and Cognitive Research, Free University Amsterdam, The Netherlands)) were grown in 50/50 DMEM/F-12 medium (Invitrogen, Breda, The Netherlands) supplemented with 15% foetal bovine serum (FBS) and 2% penicillin/streptomycin. Medium was refreshed every 2–3 days. For calcium imaging experiments, undifferentiated SH-SY5Y cells were sub-cultured in uncoated 35 mm glass-bottom dished (glass surface 78 mm^2; MatTek, Ashland, MA) at a density of 1–1.5 $\times$ 10^6 cells/glass bottom dish. Ca^{2+} measurements were performed 1–2 days after seeding. For cell viability experiments, SH-SY5Y cells were sub-cultured in 24-wells plates (Greiner Bio-one, Solingen, Germany) at a density of 2 $\times$ 10^5 cells/well.

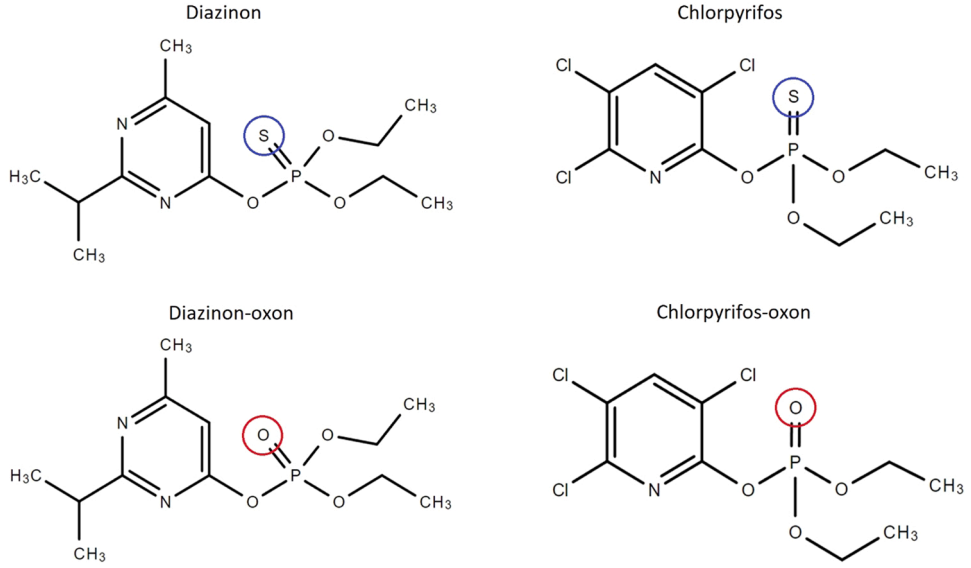

Fig. 1. Molecular structures of diazinon (CAS: 333–41–5; top-left), diazinon-oxon (CAS: 962–58–3; bottom left), chlorpyrifos (CAS: 2921–88–2; top right) chlorpyrifos-oxon (CAS: 5598–15–2; bottom right).

Cortical cells were isolated from the cortex of Wistar rat pups at postnatal day 0–1 as described previously (Dingemans et al., 2016; Gerber et al., 2021) with minor modifications. Briefly, rat pups were decapitated and the cortex was isolated and placed in ice-cold dissection medium (500 mL Neurobasal A (NBA) medium, supplemented with 14 g sucrose, 1.25 mL L-glutamine (200 mM), 5 mL glutamate (3.5 mM), 5 mL penicillin/streptomycin, 50 mL FBS and pH adjusted to 7.4). Cortices were minced and triturated to a homogenous suspension and filtered through an easy strainer (100 μm, Greiner Bio One, Alphen aan den Rijn, The Netherlands). Subsequently, cells were centrifuged for 5 min at 800 rpm. The supernatant was removed and the pellet was resuspended using 1 mL of dissection medium per rat brain and diluted to a cell suspension containing 2×10^6 cells/mL. For calcium imaging experiments, cells were seeded in glass-bottom dishes in 2.5 mL dissection medium at a density of 4×10^5 cells/dish. For cell viability experiments, cells were seeded in 48-wells plates (Greiner Bio-one, Solingen, Germany) at a density of 2×10^5 cells/well. For MEA experiments, a 50 μL drop of cell suspension (1×10^5 cells/well) was placed on the electrode field in each well of the 48-wells microelectrode array plate (MEA, Axion BioSystems Inc, Atlanta, USA, M768-GL1–30Pt200). Cultures were maintained in a humidified 5% CO_2/95% air atmosphere at 37 °C for 2 h, after which 450 μL dissection medium was added to each well. All cell culture material for primary cortical cultures was coated with 0.1% polyethyleneimine (PEI) for 1 h. For the mwMEA plates, the day following plating (one day in vitro (DIV1)), 450 μL dissection medium was replaced by 450 μL glutamate medium (450 mL NBA medium, 14 g sucrose, 1.25 mL L-glutamine (200 mM), 5 mL glutamate (3.5 mM), 5 mL penicillin/streptomycin and 10 mL B-27, pH 7.4). At four days in vitro (DIV4), 450 μL glutamate medium was replaced by 450 μL FBS medium (450 mL NBA medium, 14 g sucrose, 1.25 mL L-glutamine (200 mM), 5 mL Penicillin/streptomycin and 50 mL FBS, pH 7.4). For maintenance of the culture, a 50% medium change was applied every 3–4 days.

Animal experiments were performed in agreement with Dutch law, the European Community directives regulating animal research (2010/63/EU) and approved by the Ethical Committee for Animal Experiments of Utrecht University. All efforts were made to minimize the number of animals used and their suffering.

2.3. Cell viability assay

Effects of test compounds on cell viability in rat primary cortical cultures and SH-SY5Y cells were assessed using the Alamar Blue (AB) assay (protocol adapted from Bopp and Lettieri, 2007). Cells were exposed to a range of concentrations up to 100 μM for 48 h (SH-SY5Y) or 48 h and 14 days (primary cortical cultures). Mitochondrial activity of the cells was recorded as a measure of cell viability with the AB assay, which is based on the ability of the cells to reduce resazurin to resorufin. Briefly, following exposure, cells were incubated for 30 min with 12,5 μM AB solution in HBSS (Invitrogen, Breda, The Netherlands). Resorufin was measured spectrophotometrically at 540/590 nm (Infinite M200 microplate; Tecan Trading AG, Männedorf, Switzerland).

2.4. Calcium imaging

Changes in $[Ca^{2+}]_i$ were measured on a single-cell level using the Ca^{2+}-sensitive, fluorescent ratio dye Fura-2 AM as described previously (Heusinkveld et al., 2013; Meijer et al., 2014b). Briefly, cells were loaded with 5 μM Fura-2 AM (Molecular Probes; Invitrogen, Breda, The Netherlands) for 20 min at room temperature, followed by 15 min de-esterification. After de-esterification, the cells were placed on the stage of an Observer A1 inverted microscope (Zeiss, Göttingen, Germany) equipped with a Lambda DG-4 illumination system (Sutter Instrument Company, Novato CA, USA). Fluorescence, evoked by 340 and 380 nm excitation wavelengths (F340 and F380), was collected every 3 s at 510 nm with a CoolSNAP™ MYO CCD camera (Photometrics, Tucson, AZ, USA). To investigate compound-induced effects on depolarization-evoked $[Ca^{2+}]_i$, cells were depolarized by switching superfusion from saline to high-K^+ containing saline (100 mM K^+, Na^+ lowered to 30 mM to maintain osmolarity) for 18 s after a 5 min baseline recording. This depolarization to ~0 mV adequately opens both high and low voltage-activated calcium channels. Following a ~10 min recovery period, cells were exposed to DMSO (0.1%) or one of the test compounds for 20 min. Subsequently, cells were depolarized for a second time to evaluate effects of exposure on depolarization-evoked Ca^{2+}-influx. This is calculated as the treatment ratio (TR; in %) between the first and second depolarization-evoked $[Ca^{2+}]_i$ peak values relative to control.

2.5. MEA recordings

Multi-well MEA plates contain 48-wells per plate, with each well containing 16 individual embedded nanotextured gold microelectrodes, yielding a total of 768 channels (Axion Biosystems Inc.). Recordings were made as previously described (Dingemans et al., 2016; Gerber et al., 2021). Both OP-insecticides and their respective –oxon metabolites were tested at final concentrations of 0.1–100 μM in acute MEA experiments, whereas the concentration range was extended to 0.001 μM for chronic exposure. Each well was exposed to only one condition (i.e. one concentration of a test compound) to prevent potential effects of cumulative dosing, such as receptor (de)sensitization.

For acute MEA experiments on DIV 9–11, a 48-wells mwMEA plate was placed into the Maestro 768-channel amplifier with integrated heating system, temperature controller and data acquisition interface (Axion BioSystems Inc, Atlanta, USA). After a 5 min stabilization period at 37 °C, a 30 min baseline recording of spontaneous activity was started. Wells with at least four bursting electrodes at baseline recording were included for experiments. After the baseline recording, a 40 min exposure recording was started to determine the acute (30 min exposure) effects of different substances. During the first 5 min of the exposure recording, all active wells were exposed individually to test compounds by manually pipetting 5 μL of stock solution containing the test substance to each active well. At DIV 10 and DIV 11, neuronal activity was measured again for 30 min to check for effects after respectively 24 h and 48 h of exposure.

For chronic (10 days) MEA experiments, a 30 min baseline recording was performed on DIV 7, since at DIV 7, neuronal networks have started developing and spontaneous network activity can be measured (Dingemans et al., 2016). Wells with at least four bursting electrodes at baseline recording were included for experiments. After the baseline recording, a half medium change was performed to expose the cells to the desired concentration of the test compound. During the half medium change, the medium was first resuspended, after which half the medium (250 μL) was removed. This was replaced by 250 μL fresh medium containing the desired exposure concentration of the test compound. At DIV 10, 14 and 17 another 30 min MEA recording was performed, followed by a half medium change. After the final MEA measurement, cell viability was assessed using the Alamar Blue assay.

All conditions were tested on neuronal cultures originating from at least 3 different isolations, in at least 3 plates and at least 9 wells for acute MEA experiments and at least 4 plates and at least 16 wells for chronic MEA experiments. The number of wells represents the number of replicates per condition.

3. Data analysis and statistics

Data from cell viability experiments in the rat primary cortex (48 h and 14d of exposure) and human SH-SY5Y cells (48 h of exposure) is derived from 2 to 4 individual experiments ($N \geq 2$) consisting of 6 biological replicates per experiment ($n = 12–18$ wells).

Data from single-cell fluorescence microscopy is presented as F340/F380 ratio (R), reflecting changes in $[Ca^{2+}]_i$, and analyzed using custom-made MS-Excel macros applying a correction for background fluorescence (Heusinkveld et al., 2013). The treatment ratio (TR) represents the second depolarization-evoked increase in $[Ca^{2+}]_i$ in treated cells as a percentage of the response to the first depolarization, expressed relative to the TR in control cells. The data represent average values derived from 17 - 81 individual cells (n) from at least 4 independent experiments (N).

Data analysis for the MEA data was done as described in (Gerber et al., 2021). Briefly, MEA data acquisition was performed using Axion's Integrated Studio (AxIS 1.7.8) and channels were sampled at 12.5 kHz. Signals were pre-amplified with a gain of 1200 × and band-pass filtered at 200–5000 Hz. This raw data was pre-processed to obtain.spk files. Spikes were detected using the AxIS spike detector (Adaptive threshold crossing, Ada BandFlt v2) with a post/pre spike duration of 3.6/2.4 ms and a spike threshold of 7 × SD of the internal noise level (rms) of each individual electrode. Spike information was then further analysed using NeuralMetrics Tool (v 3.1.7, Axion BioSystems) and custom-made macros in Excel. Bursts were defined using the Poisson surprise method (Legendy and Salcman, 1985) with a minimum of 10 surprises. Network bursts were defined using an adaptive threshold with a minimum of 40 spikes, each separated by a maximum interval set automatically on a well-by-well basis based on the mean spike rate of each well, for a minimum of 15% of the electrodes/well. Data from the last 10 min of the 40 min exposure recordings (acute MEA) or last 20 min of each 30 min recording (chronic MEA) were used for analysis, since this is the most stable timeframe for stable exposure effects (see (Hondebrink et al., 2016). Acute MEA data are presented as percentage change compared to baseline, relative to control (treatment ratio). While many parameters can be extracted from MEA data, our analysis focused on the number of spikes, bursts and network bursts. The data represent average values derived from 9 to 21 wells (*n*) from 3 to 4 independent experiments (*N*). Chronic MEA data (DIV 7–17 exposure) are presented as percentage change compared to the time-matched control per plate (treatment ratio). The data represent average values derived from 16 to 37 wells (*n*) from 4 to 7 independent experiments (*N*).

All data are presented as mean % ± standard error of the mean (SEM) compared to solvent control. Experimental values that exceeded mean ± 2x SD (of their respective condition) were excluded since these can be considered to be outliers (<5% outliers). Benchmark response (BMR) cut-offs were based on the average variation in all pooled DMSO control experiments per exposure duration. Since differences in the variation in control experiments per exposure duration differed only marginally for the different parameters (NoSP, NoB and NoNB), a single rounded BMR value was chosen per exposure duration (see Table S1 for exact values and selected BMR values). Effects that are smaller than the BMR are considered to be of limited toxicological relevance, even if significantly different from control (indicated with asterisks). Statistical analyses were performed using GraphPad Prism v9.2.0 (GraphPad Software, San Diego, California, USA) using one-way ANOVA (cell viability and calcium imaging) and two-way (repeated measures) ANOVA (acute and chronic MEA). A p-value ≤ 0.05 was considered statistically significant. Concentration-response curves were fitted using a nonlinear sigmoidal or bell-shaped curve-fit when applicable.

4. Results

4.1. Effects on cell viability

To avoid that the effects of the OP-insecticides and their respective -oxon metabolites on Ca^{2+} homeostasis and network activity are simply due to a change in cell viability, all compounds used have been tested for effects on mitochondrial activity (determined using the AB assay; (Heusinkveld and Westerink, 2017) as a readout for cytotoxicity. Exposure of SH-SY5Y cells or rat cortical cultures for 48 h to 1–100 μM CPF, CPO, DZ or DZO does not affect mitochondrial activity (Fig. 2 A/B; only 100 μM) shown). When exposure of rat cortical cultures is prolonged to 14 days (DIV 7–21 exposure), only exposure to 100 μM CPO results in a near complete reduction of mitochondrial activity to 6.5 ± 2% ($N = 3$; $p < 0.001$). Exposure to concentrations of CPO < 100 μM as well as CPF, DZ and DZO does not affect mitochondrial activity (Fig. 2 C; only 100 μM shown).

4.2. Effects on depolarization-evoked increase in $[Ca^{2+}]_i$

Using rat PC12 cells, we have previously shown that acute inhibition of depolarization-evoked opening of voltage-gated Ca^{2+} channels (VGCC) is a common mode of action for several insecticides, including OP-insecticides (Meijer et al., 2014a, 2014b). To further generalize these findings and shed light on potential interspecies differences, we now

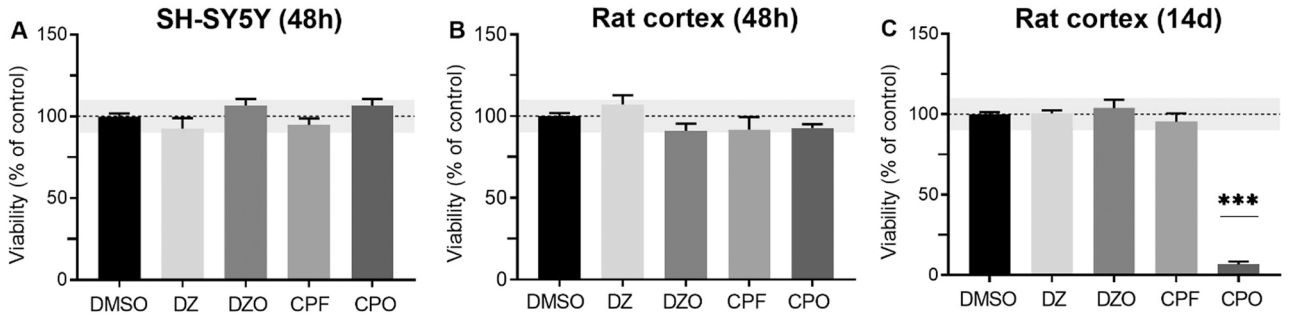

Fig. 2. Exposure of SH-SY5Y cells (A) or rat primary cortical cultures (B) for 48 h to up to 100 μM DZ, DZO, CPF and CPO does not lead to changes in cell viability. Following 14 day exposure of primary cortical cultures (DIV 7–21) only 100 μM CPO induces a decrease in cell viability (C). Concentrations of CPO < 100 μM are without effect on mitochondrial activity (not shown). The grey shaded area represents a benchmark response of 10%, which is derived from the average variation in DMSO control experiments. Bars represent the average percentage viability (± SEM; ≥ 12 wells from ≥ 2 independent experiments) compared to control. Difference from control * ** $p \leq 0.001$.

assessed the acute effects of CPF, CPO, DZ and DZO on depolarization-evoked opening of VGCC using rat primary cortical cultures and human SH-SY5Y cells (see Fig. S1 for examples of raw traces of the intracellular calcium concentration in individual cells).

Acute exposure to diazinon (DZ) results in a concentration-dependent decrease in depolarization-evoked Ca^{2+} influx in both rat cortical cultures and human SH-SY5Y cells (IC_{50} rat cortex: 66.7 μM; SH-SY5Y: 7.2 μM; Fig. 3A). Upon exposure to CPF, a concentration-dependent decrease in the depolarization-evoked Ca^{2+} influx is observed only in human SH-SY5Y cells (Fig. 3B; IC_{50}: 2.1 μM), whereas no effect of CPF could be observed in rat cortical cultures. Exposure to the -oxon metabolite of diazinon (DZO) causes a partial, but significant, decrease at the highest exposure concentration only in SH-SY5Y cells (100 μM; 65 ± 5%; Fig. 3C; IC_{50} >100 μM). On the other hand, exposure to CPO results in a concentration-dependent decrease in depolarization-evoked Ca^{2+} influx in both rat cortical cultures and human SH-SY5Y cells (IC_{50} respectively >100 μM and 12.7 μM; Fig. 3D). In general, depolarization-evoked Ca^{2+} influx is affected more and/or at lower concentrations in human SH-SY5Y cells than in rat cortical cultures after acute exposure to OP-insecticides. Furthermore, the -oxon metabolites are less potent in inhibiting depolarization-evoked Ca^{2+} influx than the respective parent compounds.

To exclude that the effects are (indirectly) mediated by the inhibition of AChE, which is the primary target of OP metabolites (Richardson et al., 2019), depolarization-evoked Ca^{2+} influx was assessed in both SH-SY5Y cells and primary cortical cells after exposure to 10 μM rivastigmine (a potent and selective AChE inhibitor (Ezzat et al., 2021)) and after co-exposure to 10 μM CPO and 10 μM rivastigmine. Rivastigmine alone has no effect on depolarization-evoked Ca^{2+} influx nor does it affect the inhibition evoked by CPO exposure (see Supplementary data Fig. S2), indicating that inhibition of AChE does not play a role in the observed inhibition of depolarization-evoked Ca^{2+} influx.

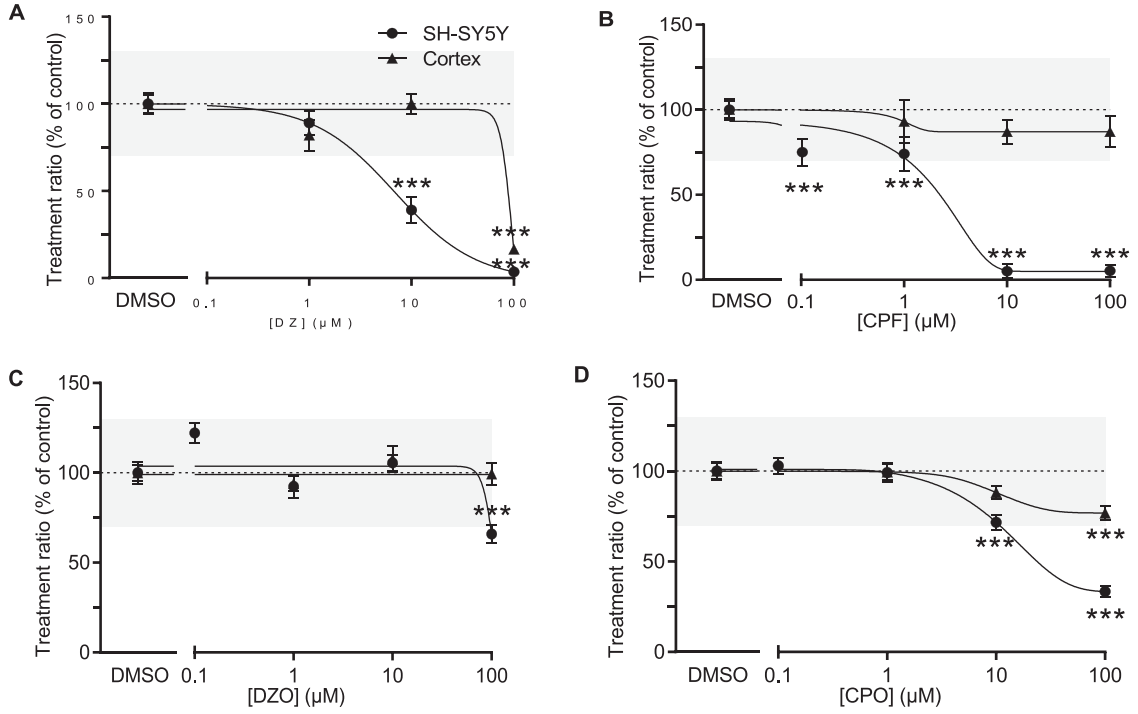

Fig. 3. Exposure to DZ (A), CPF (B), DZO (C), and CPO (D) concentration-dependently inhibits depolarization-evoked Ca^{2+} influx. The grey shaded area represents a benchmark response of 30%, which is derived from the average variation in DMSO control experiments. Data points display average percentage compared to control (DMSO control set to 100%) ± SEM from 17 to 81 individual cells (≥ 4 independent experiments per concentration). Difference from DMSO control (*** $p \leq 0.001$).

4.3. Acute effects on neuronal network activity

Next, the effects of acute exposure to DZ, CPF and their respective -oxon metabolites on spontaneous neuronal network activity were assessed using MEA recordings in rat primary cortical cultures. Acute (30 min) exposure to DZ results in a concentration-dependent decrease in number of spikes (IC_{50} 19.3 μM), bursts (IC_{50} 37.7 μM) and network bursts (IC_{50} 32.5 μM; Fig. 4A), whereas no conclusive effects of exposure to the oxon-metabolite of diazinon (DZO) could be observed on these parameters (Fig. 4C). Acute exposure to both CPF and its oxon-metabolite (CPO) results in a concentration-dependent decrease in number of spikes (IC_{50} CPF: 16.7 μM; IC_{50} CPO: 21.5 μM), bursts (IC_{50} CPF: 40.4 μM; IC_{50} CPO:15.6 μM) and network bursts (IC_{50} CPF: 12.5 μM; IC_{50} CPO: 14.1 μM; Fig. 4B and D).

After 24 and 48 h of exposure, the concentration-dependent effects for DZ are almost absent, while exposure to DZO has no obvious effect on spontaneous neuronal network activity after 24 and 48 h. IC_{50} values for CPF do not differ much between exposure durations 30 min, 24 h and 48 h, while for CPO the effects become less pronounced (see Table 1, Fig. 5 and Supplementary data Fig. S3).

To exclude that the effects on spontaneous electrical activity are caused by the inhibition of AChE, effects of rivastigmine on spontaneous neuronal activity were investigated. Rivastigmine at 1 μM and 10 μM has no effect on the number of spikes, bursts and network bursts after 30 min, 24 h and 48 h exposure, except for a modest increase in the number of network bursts after 30 min (see Supplementary data Fig. S4), clearly indicating that inhibition of AChE does not play a role in the observed decrease in neuronal network activity following exposure to DZ, CPF and CPO.

Table 1
Overview of IC_{50} values (in μM) for the OP-insecticides and their oxon-metabolites on the number of spikes (NoSP), the number of bursts (NoB) and the number of network bursts (NoNB) derived from MEA recordings after 30 min, 24 h and 48 h of exposure.

IC_{50} (μM) (NoSP; NoB; NoNB)	After 30 min	After 24 h	After 48 h
Diazinon	19.3; 37.7; 32.5	57.5; 51.3; 59.9	93.1; 90.6; 87.7
Diazinon-oxon	–	–	–
Chlorpyrifos	16.7; 40.4; 12.5	14.6; 14.5; 15.0	19.0; 19.2; 34.4
Chlorpyrifos-oxon	21.5; 15.6; 14.1	49.5; 28.9; 33.5	47.8; 40.1; 29.2

4.4. Effects of developmental exposure on network activity

Acute exposure to DZ, CPF and CPO can affect spontaneous neuronal activity after an exposure duration up to 48 h (Figs. 4–5). Since chronic, repeated exposure is more reminiscent of the human situation and exposure to OP-insecticides can also induce developmental neurotoxicity (Todd et al., 2020), we determined the effect of chronic exposure to DZ, CPF and their respective -oxon metabolites on neuronal network development and maturation. Rat primary cortical cultures were exposed for 10 days (DIV 7 – 17) to 0.001–100 μM of DZ, DZO, CPF and CPO and neuronal activity was measured at five different timepoints during development.

The results demonstrate that exposure to DZ at 100 μM has a small effect on network activity at DIV 10 that disappeared over time, while DZO has no effect on the development of spontaneous electrical network activity (as measured by the number of spikes (NoSP), bursts (NoB) and network bursts (NoNB); Fig. 6A and C). Exposure to 1 and 100, but not 10 μM CPF results in a significant, concentration-dependent decrease in

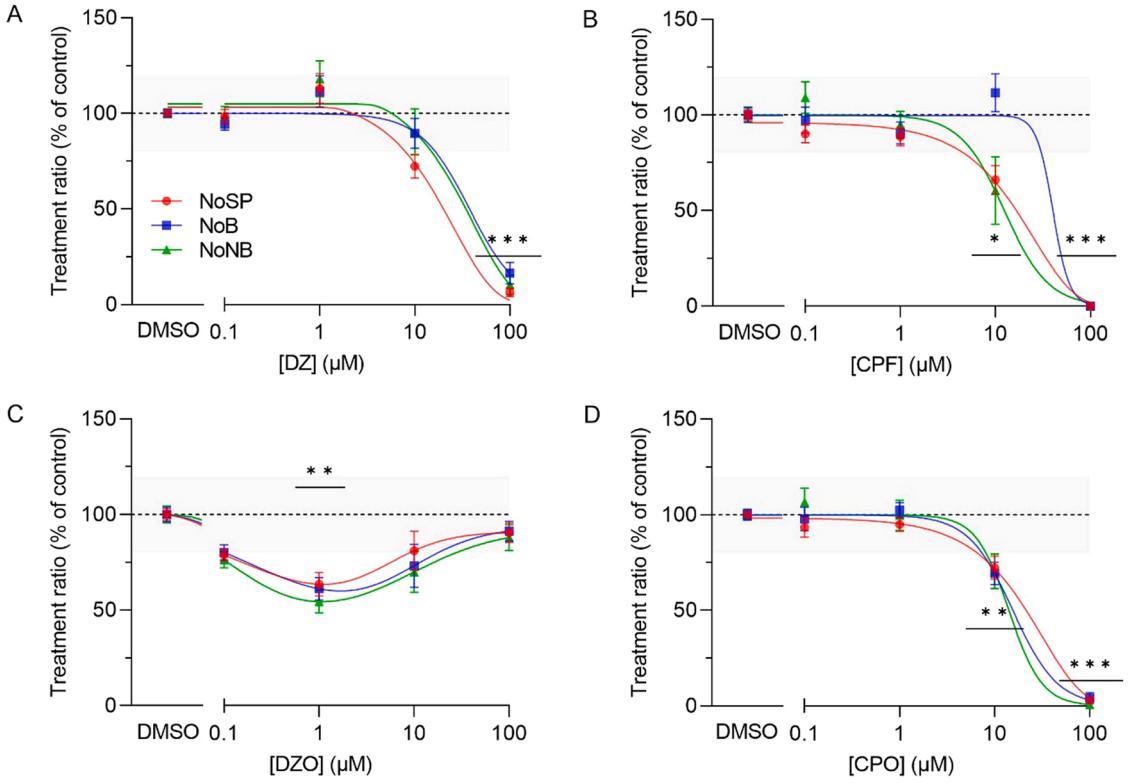

Fig. 4. Concentration-response curves for DZ (A), CPF (B), DZO (C), and CPO (D) on neuronal network activity in rat cortical cells as measured during acute 30 min exposure on the MEA. The grey shaded area represents a benchmark response of 20%, which is derived from the average variation in control experiments after 30 min of exposure. Effects on number of spikes (NoSP), bursts (NoB) and network bursts (NoNB) are depicted as average % compared to control (DMSO control set to 100%) ± SEM, from at least 9 individual wells (≥ 3 independent experiments per concentration). Difference from solvent control (* $p \leq 0.05$; ** $p \leq 0.01$; *** $p \leq 0.001$). Color of asterisks indicates which parameter is significantly affected (red for NoSP; blue for NoB; green for NoNB). Black asterisks indicate all parameters differ significant from solvent control.

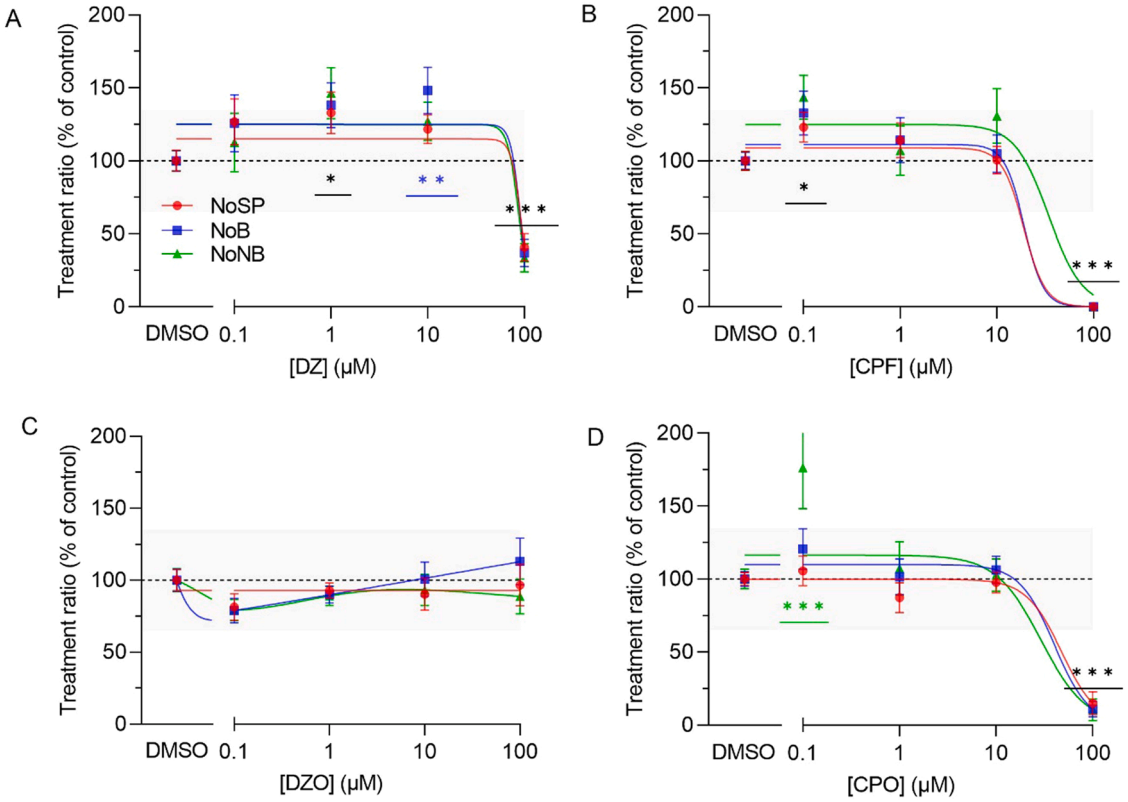

Fig. 5. Concentration-response curves for DZ (A), CPF (B), DZO (C), and CPO (D) on neuronal network activity in rat cortical cells as measured after 48 h of exposure on the MEA. The grey shaded area represents a benchmark response of 35%, which is derived from the average variation in control experiments after 48 h of exposure. Effects on number of spikes (NoSP), bursts (NoB) and network bursts (NoNB) are depicted as average % compared to control (DMSO control set to 100%) ± SEM from at least 9 individual wells (≥ 3 independent experiments per concentration). Difference from solvent control (* $p \leq 0.05$; ** $p \leq 0.01$; *** $p \leq 0.001$). Color of asterisks indicates which parameter is significantly affected (red for NoSP; blue for NoB; green for NoNB). Black asterisks indicate all parameters differ significant from solvent control.

network activity over time on all three parameters, whereas exposure to 0.1 μM CPF significantly decreases only the number of network bursts. Exposure to the lowest concentration (0.001 μM) CPF seems to gradually increase neuronal (network) activity over time, although this effect was not significant.

Finally, exposure to CPO at 100 μM results in a profound inhibition of spontaneous neuronal activity on all three parameters over time (Fig. 6D). At lower concentrations, exposure to CPO evokes a gradual increase in number of bursts over time, but this effect was not significant.

5. Discussion

Exposure to OP-insecticides and their -oxon metabolites does not induce overt cytotoxicity after 48 h in rat cortical cells and human SH-SY5Y cells. After 21 days exposure of rat cortical cells, only exposure to 100 μM CPO strongly decreases cell viability, while CPF, DZ and DZO are without effect (Fig. 2). However, the concentration at which cytotoxicity is observed lacks toxicological relevance and these findings indicate that effects on functional endpoints observed at ≤ 100 μM (for CPO ≤ 10 μM) are not confounded by cytotoxicity.

Previous studies have shown that AChE inhibition is most sensitive for the oxon metabolites of the OP-insecticides (CPO and DZO), with IC_{50} values around 0.01 μM for CPO (Gao et al., 2017; Kasteel et al., 2020; Meek et al., 2021) and ranging from 0.05 to 1 μM for DZO (Kasteel et al., 2020; Meek et al., 2021; Zhao et al., 2021). IC_{50} for both CPF and DZ are much higher and are usually in the high micromolar range (Gao et al., 2017; Meijer et al., 2014b; Rush et al., 2010; Zhao et al., 2021); see also Table 2. The current study indicates that parent OP-insecticides (CPF and DZ) can inhibit VGCCs and neuronal activity at concentrations far below their sensitivity for AChE inhibition. In line with an earlier study using PC12 cells (Meijer et al., 2014b), CPF almost completely inhibits depolarization-evoked Ca^{2+} influx via VGCC at 10 μM in human SH-SY5Y cells. In contrast, at 10 μM CPF, calcium influx in rat primary cortical cultures was inhibited only by ~20% (Meijer et al., 2015) and in line with the current data that also shows a ~25% inhibition after acute exposure to CPF at 10 μM (Fig. 3). So, these studies not only show that the effects are quite consistent and reproducible, it also shows that PC12 cells and SH-SY5Y cells seem to be much more sensitive to CPF than rat primary cortical cells. Interestingly, CPO at 10 μM induced a ~30% inhibition in PC12 cells (Meijer et al., 2014a), rat primary cortical cultures (Meijer et al., 2015) and SH-SY5Y cells (Fig. 3), and a ~20% inhibition in rat primary cortical cultures (Fig. 3). The oxon-metabolite thus seems roughly equipotent throughout the different studies regardless of the cell type. DZ and DZO also inhibit depolarization-evoked Ca^{2+} influx via VGCC, further implicating that VGCC inhibition is a common mode of action of OP insecticides and their metabolites. Notably in this respect, and in line with (Meijer et al., 2014a), parent compounds are more potent than their oxon metabolites (Table 2).

Human SH-SY5Y cells are thus more sensitive to OP-insecticide exposure than rat cortical cells. Although both cell types show robust calcium transients upon depolarization (also see Fig. S1), it is very well possible that the differences in sensitivity are due to differences in VGCC expression between cell models (Heusinkveld and Westerink, 2017). Earlier studies by (Meijer et al., 2015, 2014a) also tested the effects of CPF and CPO exposure on Ca^{2+} influx, both in the rat PC12 cell line and rat primary cortical cells. These studies showed that primary cortical

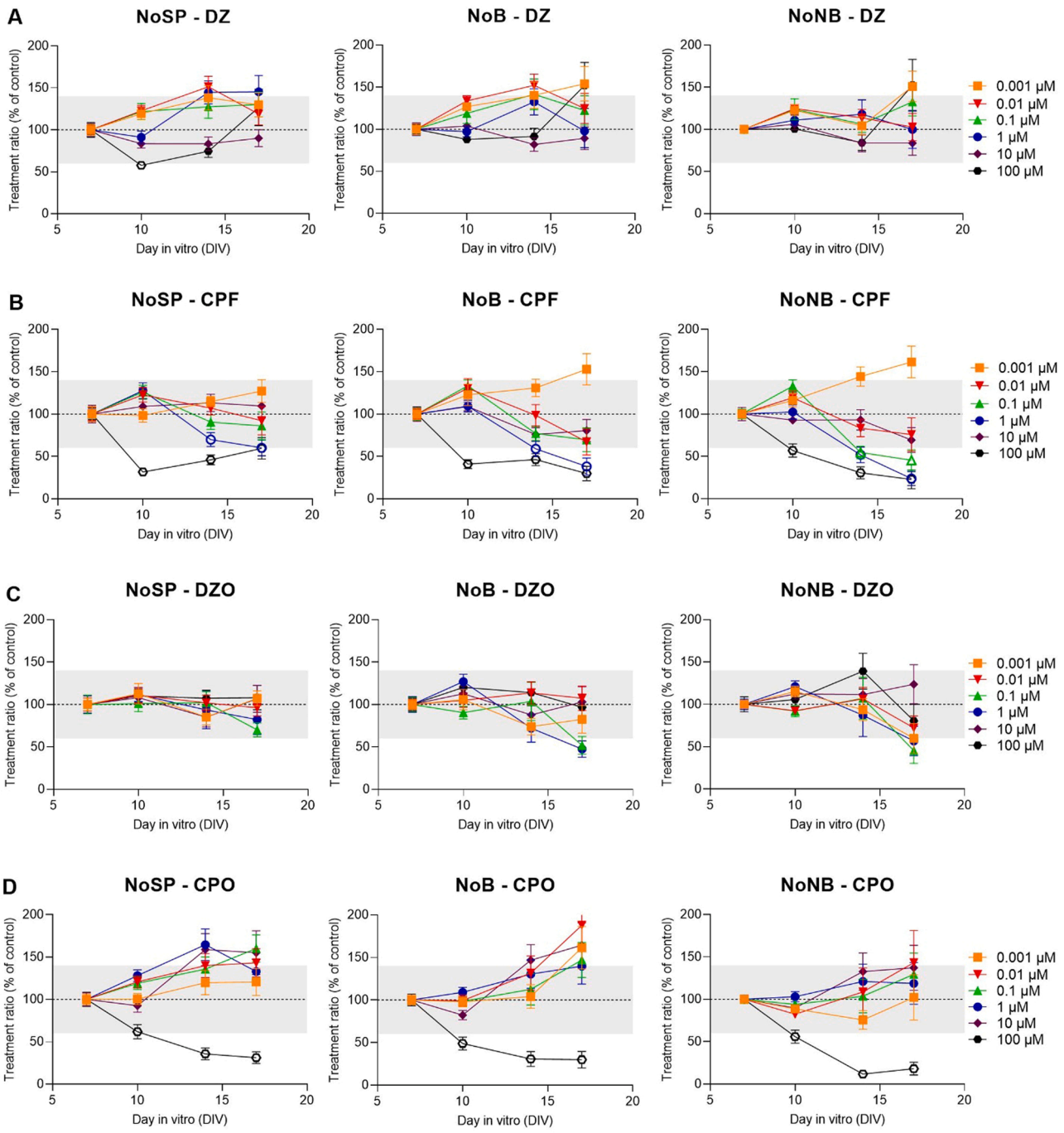

Fig. 6. Concentration-response relationships for DZ (A), CPF (B), DZO (C) and CPO (D) for number of spikes (NoSP; left), bursts (NoB; middle), and network bursts (NoNB; right) over time as measured during chronic (DIV 7–17) MEA experiments. The grey shaded area represents a benchmark response of 40%, which is derived from the average variation in control experiments at baseline (DIV7). Effects are depicted as average % change compared to time-matched control (DMSO control set to 100%) ± SEM from at least 16 individual wells (≥ 4 independent experiments per concentration). Open dots represent datapoints with a significant difference compared to solvent control ($p \leq 0.05$), whereas closed dots represent datapoints that are not significantly different compared to control.

cells were less sensitive to the effects of insecticides on VGCCs than PC12 cells. Interestingly, the results found in PC12 cells are in line with our results in the human SH-SY5Y cell line, with a concentration-dependent decrease in Ca^{2+} influx starting from 0.1 µM for both CPF and CPO, and a stronger inhibition at high micromolar concentrations for CPF than for CPO.

In PC12 cells, blocking N-type or P/Q-type VGCC inhibited calcium influx by ~20–30% (Dingemans et al., 2009), which is comparable to the inhibition seen in our data after exposure to CPF and CPO (Fig. 3). It is therefore tempting to speculate about the involvement of either N-type or P/Q-type VGCC in the observed inhibition. However, since SH-SY5Y cells do not express P/Q-type VGCC (Heusinkveld and Westerink, 2017), it could be hypothesized that inhibition of N-type VGCC, which are expressed in both SH-SY5Y and PC12 cells, is responsible for the inhibition seen after exposure to CPF and CPO although additional experiments are required to proof this hypothesis.

The hypothesized involvement of specific VGCC in the different cell models also suggests that the difference in our results between the rat cortical culture and human SH-SY5Y cells is a difference between cell models and not so much between species. As the primary cortical culture

Table 2
Overview IC_{50} values for the OP-insecticides and their oxon-metabolites on AChE inhibition derived from literature, cytotoxicity in human SY-SY5Y cells (48 h exposure) and rat primary cortical neurons (48 h and 21 days exposure), depolarization-evoked Ca^{2+} influx via VGCC in human SY-SY5Y cells and rat primary cortical neurons, spontaneous neuronal activity in rat primary cortical cultures after acute exposure (NoSP after 30 min) and developmental exposure (DIV 7–17; LOEC).

IC_{50} (μM)	AChE	Cytotoxicity			VGCC		Neuronal activity	
		SH-SY5Y (48 h)	rCortex (48 h)	rCortex (21d)	SH-SY5Y	rCortex	Acute	Developmental
Diazinon	> 10	> 100	> 100	> 100	7.2	66.7	19.3	> 100
Chlorpyrifos	> 50	> 100	> 100	> 100	2.1	> 100	16.7	1
Diazinon-oxon	0.05	> 100	> 100	> 100	> 100	> 100	> 100	> 100
Chlorpyrifos-oxon	0.01	> 100	> 100	100	12.7	> 100	21.5	100

is a heterogeneous model comprising of multiple neuronal cell types, including glial cells such as astrocytes, this difference might also be due to the presence of potential feedback mechanisms that are not present in cell lines (Meijer et al., 2015).

Notably, the effects of OP-insecticide exposure on $[Ca^{2+}]_i$ are not AChE-mediated, since exposure to 10 μM rivastigmine (a potent and selective AChE inhibitor (Ezzat et al., 2021)) and co-exposure of 10 μM CPO and 10 μM rivastigmine has no effect on depolarization-evoked Ca^{2+} influx in SH-SY5Y cells and rat primary cortical cells.

The current study also assessed effect on neuronal network development and function using MEA recordings. Effects of acute exposure were largely in line with effects on depolarization-evoked Ca^{2+} influx, with decreases in neuronal activity observed at higher concentrations for CPF, CPO and DZ. Rat IC_{50} values for effects on neuronal activity are lower than for effects on depolarization-evoked Ca^{2+} influx (Table 2), suggesting that neuronal activity parameters are especially sensitive to OP exposure. It could be that the modest effect on Ca^{2+} influx after exposure to CPF and CPO at 10–100 μM is already sufficient to cause a full inhibition of neuronal activity. Another possibility is that other targets involved in neuronal transmission, such as the glutamatergic AMPA receptor, the $GABA_A$ receptor or the GABA transporter, are also affected at this (high) micromolar range (Alugubelly et al., 2021; Torres-Altoro et al., 2011). The decrease in neuronal activity found here is reflected in a decrease in the number of spikes, bursts and network bursts. These effects are not AChE-mediated since exposure to 10 μM rivastigmine did not decrease neuronal network activity. Notably, exposure to DZO also had no effect on neuronal activity and $[Ca^{2+}]_i$. Although rivastigmine exposure does not decrease neuronal activity, it cannot be excluded that AChE inhibition does play a role in the decrease in neuronal activity found after OP-insecticide exposure. Notably in this respect, MEA recordings of neuronal activity from rat primary cortical cultures are not very sensitive to AChE inhibition, most likely due to the low number of cholinergic neurons and thus also very low ACh levels. Human SH-SY5Y cells appear more sensitive to the effects of OP-insecticides on VGCC. Unfortunately, however, SH-SY5Y cells do not form spontaneously active networks and are thus not compatible with MEA recordings, thereby precluding further comparison of interspecies differences. Future use of human induced pluripotent stem cells (hiPSCs) may shed light on possible species differences.

Of particular interest is that exposure to DZ showed almost no effect on neuronal activity after 48 h, while exposure to CPO had a less potent effect on neuronal activity after 24 h and 48 h. Exposure to CPF, on the contrary, did not differ in potency over time. This suggests that the neurotoxicity after exposure to different OPs has different effects over time. The differences in effects between CPF and CPO was mirrored in Ca^{2+} influx results found by Meijer et al. (2015) in PC12 cells, where 24 h exposure to CPF had a stronger effect than exposure to CPO. The decrease in potency on neuronal activity for DZ and CPO could be due to early insult and subsequent (partial) recovery of long-term network activity over time, the detoxification of the compounds and/or by desensitization of the target receptors (Gainetdinov et al., 2004).

To expand on the different effects found after prolonged exposure, the current study assessed if chronic exposure to the OP insecticides and their oxon metabolites over 10 days affected neuronal network development and maturation. Chronic exposure to both DZ and DZO had no profound effects on the development of neuronal activity over time, which is in line with the effects on neuronal activity found after 48 h exposure to these compounds. Exposure to ≥ 1 μM CPF decreased neuronal activity over time. Interestingly, exposure to even lower concentrations CPF also decreased neuronal activity, with a significant reduction in number of network bursts. Continuing exposure for a longer duration might verify if low micromolar CPF concentrations can indeed affect neuronal network activity over time, although the increase in variation in the data with increasing exposure duration (also see Table S1) may hamper the reliable detection of subtle effects. The persistent decrease in neuronal activity after CPF exposure at both 48 h and 10 days could be due to adaptive mechanisms such as gene expression, protein function and/or changes in receptor turnover (Lipscombe et al., 2013). Similar to the effects found after 48 h, CPO exposure had less potent effects than CPF exposure. Only exposure to 100 μM CPO decreased neuronal activity, but this concentration lacks toxicological relevance.

To determine if the effects detected on both Ca^{2+} influx and neuronal activity occur at relevant concentrations, we compared concentrations of OP-insecticides that inhibited VGCCs and had an effect on neuronal activity with (occupational) human exposure levels. In women and children living in an intensively farmed region, blood levels for chlorpyrifos amounted to 2,49 - 53,29 ng/mL, which relates to an estimated internal dose of 0.0071–0.152 μM. However, exposure levels as high as 5 μM have also reported and occupational exposure levels are likely to be even higher (Huen et al., 2012; Phung et al., 2012). For DZ, exposure levels in women and newborns living in an agricultural area are around 0.002 μM (Huen et al., 2012). The actual concentrations in the brain could differ from these values due to metabolism or barrier effects. For example, it is known that CPF not only reaches the blood-brain barrier, but also reduces its integrity (Parran et al., 2005). If this also holds for the other compounds investigated here is not known. It is likely that parent OPs, such as CPF and DZ persist longer in the human body than their oxon-metabolites and thus play a more prominent role.

Notably, young animals/humans have a lower rate of OP metabolism (Eaton et al., 2008) and as a result, the parent compounds may persist longer in young animals/humans. The relative contribution of the parent compound to the toxic effect can thus also be more prominent. From a risk assessment perspective it is important to point out that toddlers were estimated to have the highest daily intake per kg bw of chlorpyrifos compared to infants and adults (Eaton et al., 2008).

Our data demonstrate that parent OPs CPF and DZ have more profound effects on both Ca^{2+} influx and neuronal activity than CPO and DZO. CPF even has an effect on neuronal network development, illustrating the need to investigate possible links between early-life OP exposure and neurodevelopmental disorders in children. Future studies can expand on this by extending the exposure duration to 28 days and using hiPSCs to better match the real life situation in humans. In conclusion, our findings demonstrate the importance of non-AChE mediated mechanisms of neurotoxicity after OP exposure.

CRediT authorship contribution statement

Lennart V.J. van Melis: Conceptualization, Formal analysis, Writing – original draft, Writing – review & editing. **Harm J. Heusinkveld:** Conceptualization, Investigation, Formal analysis, Supervision, Writing – original draft, Project administration. **Celine Langendoen:** Investigation, Formal analysis. **Anouk Peters:** Investigation, Formal analysis. **Remco H.S. Westerink:** Conceptualization, Writing – original draft, Writing – review & editing, Supervision, Project administration, Funding acquisition.

Declaration of Competing Interest

The authors declare that they have no known competing financial interests or personal relationships that could have appeared to influence the work reported in this paper.

Data availability

Data will be made available on request.

Acknowledgments

We are grateful to Aart de Groot and Gina van Kleef for expert technical assistance. This work was funded by the Dutch-German (ZonMW-BMBF) funded project N3rvousSystem (Grant #114027001), the European Union's Horizon 2020 funded project ENDpoiNTs (Grant #825759), and the Faculty of Veterinary Medicine (Utrecht University). The authors declare they have no competing financial interests.

Conflict of interest

The authors declare that there are no conflicts of interest. Given his role as Editor in Chief of NeuroToxicology, Remco H.S. Westerink had no involvement in the peer-review of this article and has no access to information regarding its peer-review. Full responsibility for the editorial process for this article was delegated to Dr. Pamela J. Lein.

Appendix A. Supporting information

Supplementary data associated with this article can be found in the online version at doi:10.1016/j.neuro.2022.11.002.

References

Alugubelly, N., Mohammed, A.N., Carr, R.L., 2021. Persistent proteomic changes in glutamatergic and GABAergic signaling in the amygdala of adolescent rats exposed to chlorpyrifos as juveniles. Neurotoxicology 85, 234–244. https://doi.org/10.1016/j.neuro.2021.05.012.

Biedler, J.L., Helson, L., Spengler, B.A., 1973. Morphology and growth, tumorigenicity, and cytogenetics of human neuroblastoma cells in continuous culture. Cancer Res 33, 2643–2652. https://doi.org/10.1007/PL00000826.

Casida, J.E., 2017. Organophosphorus xenobiotic toxicology. Annu Rev. Pharm. Toxicol. 57, 309–327. https://doi.org/10.1146/annurev-pharmtox-010716-104926.

Chin-Chan, M., Navarro-Yepes, J., Quintanilla-Vega, B., 2015. Environmental pollutants as risk factors for neurodegenerative disorders: Alzheimer and Parkinson diseases. Front Cell Neurosci. 9, 124. https://doi.org/10.3389/fncel.2015.00124.

Christen, V., Rusconi, M., Crettaz, P., Fent, K., 2017. Developmental neurotoxicity of different pesticides in PC-12 cells in vitro. Toxicol. Appl. Pharm. 325, 25–36. https://doi.org/10.1016/j.taap.2017.03.027.

Cotterill, E., Hall, D., Wallace, K., Mundy, W.R., Eglen, S.J., Shafer, T.J., 2016. Characterization of early cortical neural network development in multiwell microelectrode array plates. J. Biomol. Screen 21, 510–519. https://doi.org/10.1177/1087057116640520.

Das, K.P., Barone, S., 1999. Neuronal differentiation in PC12 cells is inhibited by chlorpyrifos and its metabolites: Is acetylcholinesterase inhibition the site of action. Toxicol. Appl. Pharm. 160, 217–230. https://doi.org/10.1006/taap.1999.8767.

Dingemans, M.M.L., Heusinkveld, H.J., de Groot, A., Bergman, Å., van den Berg, M., Westerink, R.H.S., 2009. Hexabromocyclododecane Inhibits Depolarization-Induced Increase in Intracellular Calcium Levels and Neurotransmitter Release in PC12 Cells. Toxicol. Sci. 107, 490–497. https://doi.org/10.1093/toxsci/kfn249.

Dingemans, M.M.L., Schütte, M.G., Wiersma, D.M.M., de Groot, A., van Kleef, R.G.D.M., Wijnolts, F.M.J., Westerink, R.H.S., 2016. Chronic 14-day exposure to insecticides or methylmercury modulates neuronal activity in primary rat cortical cultures. Neurotoxicology 57, 194–202. https://doi.org/10.1016/j.neuro.2016.10.002.

Dolphin, A.C., Lee, A., 2020. Presynaptic calcium channels: specialized control of synaptic neurotransmitter release. Nat. Rev. Neurosci. https://doi.org/10.1038/s41583-020-0278-2.

Eaton, D.L., Daroff, R.B., Autrup, H., Bridges, J., Buffler, P., Costa, L.G., Coyle, J., McKhann, G., Mobley, W.C., Nadel, L., Neubert, D., Schulte-Hermann, R., Spencer, P. S., 2008. Review of the toxicology of chlorpyrifos with an emphasis on human exposure and neurodevelopment. Crit. Rev. Toxicol. https://doi.org/10.1080/10408440802272158.

Ezzat, S.M., Salem, M.A., el Mahdy, N.M., Ragab, M.F., 2021. Rivastigmine. Nat. Occur. Chem. Alzheimer's Dis. 93–108. https://doi.org/10.1016/B978-0-12-819212-2.00007-4.

Flaskos, J., 2012. The developmental neurotoxicity of organophosphorus insecticides: A direct role for the oxon metabolites. Toxicol. Lett. 209, 86–93. https://doi.org/10.1016/J.TOXLET.2011.11.026.

Flaskos, J., Sachana, M., 2011. Developmental neurotoxicity of anticholinesterase pesticides. : Anticholinesterase Pestic.: Metab., Neurotox., Epidemiol. https://doi.org/10.1002/9780470640500.ch16.

Gainetdinov, R.R., Premont, R.T., Bohn, L.M., Lefkowitz, R.J., Caron, M.G., 2004. Desensitization of G protein-coupled receptors and neuronal functions. Annu Rev. Neurosci. https://doi.org/10.1146/annurev.neuro.27.070203.144206.

Gao, J., Naughton, S.X., Beck, W.D., Hernandez, C.M., Wu, G., Wei, Z., Yang, X., Bartlett, M.G., Terry, A., 2017. Chlorpyrifos and chlorpyrifos oxon impair the transport of membrane bound organelles in rat cortical axons. Neurotoxicology v (62), 111–123. https://doi.org/10.1016/J.NEURO.2017.06.003.

Gerber, L.S., van Melis, L.V.J., van Kleef, R.G.D.M., de Groot, A., Westerink, R.H.S., 2021. Culture of Rat Primary Cortical Cells for Microelectrode Array (MEA) Recordings to Screen for Acute and Developmental Neurotoxicity. Curr. Protoc. 1. https://doi.org/10.1002/cpz1.158.

Goldman, S.M., 2014. Environmental Toxins and Parkinson's Disease. Annu Rev. Pharm. Toxicol. 54, 141–164. https://doi.org/10.1146/annurev-pharmtox-011613-135937.

Heusinkveld, H.J., Westerink, R.H.S., 2017. Comparison of different in vitro cell models for the assessment of pesticide-induced dopaminergic neurotoxicity. Toxicol. Vitr. 45, 81–88. https://doi.org/10.1016/j.tiv.2017.07.030.

Heusinkveld, H.J., Molendijk, J., van den Berg, M., Westerink, R.H.S., 2013. Azole fungicides disturb intracellular Ca2+ in an additive manner in dopaminergic PC12 cells. Toxicol. Sci. 134. https://doi.org/10.1093/toxsci/kft119.

Hogberg, H.T., Sobanski, T., Novellino, A., Whelan, M., Weiss, D.G., Bal-Price, A.K., 2011. Application of micro-electrode arrays (MEAs) as an emerging technology for developmental neurotoxicity: Evaluation of domoic acid-induced effects in primary cultures of rat cortical neurons. Neurotoxicology 32, 158–168. https://doi.org/10.1016/j.neuro.2010.10.007.

Hondebrink, L., Verboven, A.H.A., Drega, W.S., Schmeink, S., de Groot, M.W.G.D.M., van Kleef, R.G.D.M., Wijnolts, F.M.J., de Groot, A., Meulenbelt, J., Westerink, R.H.S., 2016. Neurotoxicity screening of (illicit) drugs using novel methods for analysis of microelectrode array (MEA) recordings. Neurotoxicology 55, 1–9. https://doi.org/10.1016/j.neuro.2016.04.020.

Huen, K., Bradman, A., Harley, K., Yousefi, P., Boyd Barr, D., Eskenazi, B., Holland, N., 2012. Organophosphate pesticide levels in blood and urine of women and newborns living in an agricultural community. Environ. Res 117, 8–16. https://doi.org/10.1016/j.envres.2012.05.005.

Kasteel, E.E.J., Nijmeijer, S.M., Darney, K., Lautz, L.S., Dorne, J.L.C.M., Kramer, N.I., Westerink, R.H.S., 2020. Acetylcholinesterase inhibition in electric eel and human donor blood: an in vitro approach to investigate interspecies differences and human variability in toxicodynamics. Arch. Toxicol. 94, 4055–4065. https://doi.org/10.1007/s00204-020-02927-8.

Kim, K.H., Kabir, E., Jahan, S.A., 2017. Exposure to pesticides and the associated human health effects. Sci. Total Environ. https://doi.org/10.1016/j.scitotenv.2016.09.009.

Kosnik, M.B., Strickland, J.D., Marvel, S.W., Wallis, D.J., Wallace, K., Richard, A.M., Reif, D.M., Shafer, T.J., 2020. Concentration–response evaluation of ToxCast compounds for multivariate activity patterns of neural network function. Arch. Toxicol. 94, 469–484. https://doi.org/10.1007/s00204-019-02636-x.

Legendy, C.R., Salcman, M., 1985. Bursts and recurrences of bursts in the spike trains of spontaneously active striate cortex neurons. J. Neurophysiol. 53. https://doi.org/10.1152/jn.1985.53.4.926.

Lipscombe, D., Allen, S.E., Toro, C.P., 2013. Control of neuronal voltage-gated calcium ion channels from RNA to protein. Trends Neurosci. https://doi.org/10.1016/j.tins.2013.06.008.

Lopez-Suarez, L., Awabdh, S. al, Coumoul, X., Chauvet, C., 2022. The SH-SY5Y human neuroblastoma cell line, a relevant in vitro cell model for investigating neurotoxicology in human: Focus on organic pollutants. Neurotoxicology 92, 131–155. https://doi.org/10.1016/J.NEURO.2022.07.008.

McConnell, E.R., McClain, M.A., Ross, J., LeFew, W.R., Shafer, T.J., 2012. Evaluation of multi-well microelectrode arrays for neurotoxicity screening using a chemical training set. Neurotoxicology 33. https://doi.org/10.1016/j.neuro.2012.05.001.

Meek, E.C., Carr, R.L., Chambers, J.E., 2021. In vitro age-related differences in rats to organophosphates. Toxicol. Vitr. 72, 105102 https://doi.org/10.1016/J.TIV.2021.105102.

Meijer, M., Dingemans, M.M.L., van den Berg, M., Westerink, R.H.S., 2014a. Inhibition of voltage-gated calcium channels as common mode of action for (mixtures of) distinct classes of insecticides. Toxicol. Sci. 141, 103–111. https://doi.org/10.1093/toxsci/kfu110.

Meijer, M., Hamers, T., Westerink, R.H.S., 2014b. Acute disturbance of calcium homeostasis in PC12 cells as a novel mechanism of action for (sub)micromolar concentrations of organophosphate insecticides. Neurotoxicology 43, 110–116. https://doi.org/10.1016/j.neuro.2014.01.008.

Meijer, M., Brandsema, J.A.R., Nieuwenhuis, D., Wijnolts, F.M.J., Dingemans, M.M.L., Westerink, R.H.S., 2015. Inhibition of Voltage-Gated Calcium Channels After Subchronic and Repeated Exposure of PC12 Cells to Different Classes of Insecticides. Toxicol. Sci. 147, 607–617. https://doi.org/10.1093/toxsci/kfv154.

Mostafalou, S., Abdollahi, M., 2017. Pesticides: an update of human exposure and toxicity. Arch. Toxicol. 91, 549–599. https://doi.org/10.1007/s00204-016-1849-x.

Naughton, S.X., Terry, A., 2018. Neurotoxicity in acute and repeated organophosphate exposure. Toxicology v (408), 101–112. https://doi.org/10.1016/J.TOX.2018.08.011.

Oliveri, A.N., Bailey, J.M., Levin, E.D., 2015. Developmental exposure to organophosphate flame retardants causes behavioral effects in larval and adult zebrafish. Neurotoxicol Teratol. 52, 220–227. https://doi.org/10.1016/j.ntt.2015.08.008.

Parran, D.K., Magnin, G., Li, W., Jortner, B.S., Ehrich, M., 2005. Chlorpyrifos alters functional integrity and structure of an in vitro BBB model: Co-cultures of bovine endothelial cells and neonatal rat astrocytes. Neurotoxicology 26, 77–88. https://doi.org/10.1016/j.neuro.2004.07.003.

Phung, D.T., Connell, D., Miller, G., Hodge, M., Patel, R., Cheng, R., Abeyewardene, M., Chu, C., 2012. Biological monitoring of chlorpyrifos exposure to rice farmers in Vietnam. Chemosphere 87, 294–300. https://doi.org/10.1016/J.CHEMOSPHERE.2011.11.075.

Pizzurro, D.M., Dao, K., Costa, L.G., 2014. Diazinon and diazoxon impair the ability of astrocytes to foster neurite outgrowth in primary hippocampal neurons. Toxicol. Appl. Pharm. 274, 372–382. https://doi.org/10.1016/J.TAAP.2013.11.023.

Richardson, J.R., Fitsanakis, V., Westerink, R.H.S., Kanthasamy, A.G., 2019. Neurotoxicity of pesticides. Acta Neuropathol. https://doi.org/10.1007/s00401-019-02033-9.

Robinette, B.L., Harrill, J.A., Mundy, W.R., Shafer, T.J., 2011. In vitro assessment of developmental neurotoxicity: Use of microelectrode arrays to measure functional changes in neuronal network ontogeny. Front Neuroeng. 1–9. https://doi.org/10.3389/fneng.2011.00001.

Rush, T., Liu, X.Q., Hjelmhaug, J., Lobner, D., 2010. Mechanisms of chlorpyrifos and diazinon induced neurotoxicity in cortical culture. Neuroscience 166, 899–906. https://doi.org/10.1016/J.NEUROSCIENCE.2010.01.025.

Savy, C.Y., Fitchett, A.E., Blain, P.G., Morris, C.M., Judge, S.J., 2018. Gene expression analysis reveals chronic low level exposure to the pesticide diazinon affects psychological disorders gene sets in the adult rat. Toxicology 393. https://doi.org/10.1016/j.tox.2017.11.006.

Sensi, S.L., Weiss, J., Granzotto, A., Voorhees, J.R., Pieper, A.A., Rohlman, D.S., Lein, P.J., 2017. Neurotoxicity in preclinical models of occupational exposure to organophosphorus compounds. Front. Neurosci. 1, 590. https://doi.org/10.3389/fnins.2016.00590.

Sidiropoulou, E., Sachana, M., Flaskos, J., Harris, W., Hargreaves, A.J., Woldehiwet, Z., 2009. Diazinon oxon affects the differentiation of mouse N2a neuroblastoma cells. Arch. Toxicol. 83, 373–380. https://doi.org/10.1007/s00204-008-0339-1.

Slotkin, T.A., Skavicus, S., Seidler, F.J., 2017. Diazinon and parathion diverge in their effects on development of noradrenergic systems. Brain Res Bull. 130, 268–273. https://doi.org/10.1016/j.brainresbull.2017.02.004.

Strickland, J.D., Martin, M.T., Richard, A.M., Houck, K.A., Shafer, T.J., 2018. Screening the ToxCast phase II libraries for alterations in network function using cortical neurons grown on multi-well microelectrode array (mwMEA) plates. Arch. Toxicol. 92, 487–500. https://doi.org/10.1007/s00204-017-2035-5.

Todd, S.W., Lumsden, E.W., Aracava, Y., Mamczarz, J., Albuquerque, E.X., Pereira, E.F.R., 2020. Gestational exposures to organophosphorus insecticides: From acute poisoning to developmental neurotoxicity. Neuropharmacology 180, 108271. https://doi.org/10.1016/J.NEUROPHARM.2020.108271.

Torres-Altoro, M.I., Mathur, B.N., Drerup, J.M., Thomas, R., Lovinger, D.M., O'Callaghan, J.P., Bibb, J.A., 2011. Organophosphates dysregulate dopamine signaling, glutamatergic neurotransmission, and induce neuronal injury markers in striatum. J. Neurochem 119, 303–313. https://doi.org/10.1111/j.1471-4159.2011.07428.x.

Tsai, Y.H., Lein, P.J., 2021. Mechanisms of organophosphate neurotoxicity. Curr. Opin. Toxicol. 26, 49–60. https://doi.org/10.1016/J.COTOX.2021.04.002.

Tukker, A.M., Wijnolts, F.M.J., de Groot, A., Westerink, R.H.S., 2020. Applicability of hipsc-derived neuronal cocultures and rodent primary cortical cultures for in vitro seizure liability assessment. Toxicol. Sci. 178. https://doi.org/10.1093/toxsci/kfaa136.

Ubaid ur Rahman, H., Asghar, W., Nazir, W., Sandhu, M.A., Ahmed, A., Khalid, N., 2021. A comprehensive review on chlorpyrifos toxicity with special reference to endocrine disruption: Evidence of mechanisms, exposures and mitigation strategies. Sci. Total Environ. 755, 142649 https://doi.org/10.1016/J.SCITOTENV.2020.142649.

Zhang, J., Dai, H., Deng, Y., Tian, J., Zhang, C., Hu, Z., Bing, G., Zhao, L., 2015. Neonatal chlorpyrifos exposure induces loss of dopaminergic neurons in young adult rats. Toxicology 336, 17–25. https://doi.org/10.1016/j.tox.2015.07.014.

Zhao, S., Wesseling, S., Spenkelink, B., Rietjens, I.M.C.M., 2021. Physiologically based kinetic modelling based prediction of in vivo rat and human acetylcholinesterase (AChE) inhibition upon exposure to diazinon. Arch. Toxicol. 95, 1573–1593. https://doi.org/10.1007/s00204-021-03015-1.